JACS
JOURNAL OF THE AMERICAN CHEMICAL SOCIETY
Article
pubs.acs.org/JACS

# Photoinduced Electron Transfer from PbS Quantum Dots to Cobalt(III) Schiff Base Complexes: Light Activation of a Protein Inhibitor

Mark D. Peterson,[†] Robert J. Holbrook,[†,‡,§,∥] Thomas J. Meade,*[,†,‡,§,∥] and Emily A. Weiss*[,†]

[†]Department of Chemistry, Northwestern University, 2145 Sheridan Road, Evanston, Illinois 60208, United States

[‡]Department of Molecular Biosciences, Northwestern University, 2205 Tech Drive, Hogan 2100, Evanston, Illinois 60208, United States

[§]Department of Neurobiology, Northwestern University, 2205 Tech Drive, Hogan 2100, Evanston, Illinois 60208, United States

[∥]Department of Radiology, Feinberg School of Medicine, Northwestern University, 676 North St. Clair Street, Chicago, Illinois 60611, United States

Supporting Information

**ABSTRACT:** This paper describes the activation of a biologically inert Co(III) Schiff base [Co(III)-SB] complex to its protein inhibitor form by photoinduced electron transfer (PET) from a colloidal PbS quantum dot (QD, radii of 1.5−1.7 nm) to the cobalt center, with a charge separation time constant of 125 ns. Reduction of the Co(III)-SB complex initiates release of the native axial ligands, promoting replacement with the histidine mimic 4-methylimidazole. The rate of ligand displacement increases by a factor of approximately 8 upon exposure of the PbS QD/Co(III)-SB mixture to light with an energy greater than the energy of the first excitonic state of the QDs, from which PET occurs. These results suggest an approach for the preparation of inorganic therapeutic agents that can be specifically coupled to a biologically active site by cooperative redox binding ligation.

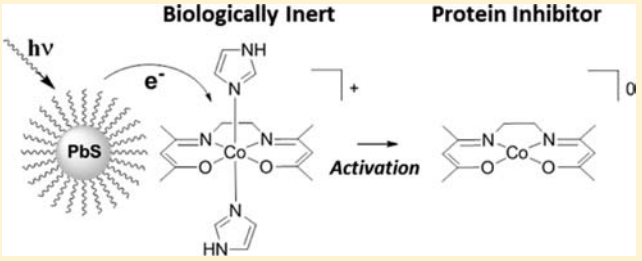


## INTRODUCTION

Recent advances in the development of therapeutic antitumor and antiviral agents have focused on compounds that bind to the biological active site of an enzyme. Although these reversibly bound drugs are susceptible to nonspecific and potentially undesirable reactions, the success of transition metal therapeutics, such as cisplatin, has refocused efforts aimed at investigating new complexes in this broad class.[1] This research has facilitated an improved understanding of the interactions between complex biological systems and inorganic coordination complexes.[2,3]

To further enhance the efficacy of transition metal inhibitors in research and clinical applications, it is crucial that precise spatial and temporal control of the activity of the agent be realized. Strategies for designing prodrugs, drugs that are administered as inactive compounds but are triggered by some controllable stimulus, have exploited differences in biological environments, such as pH, redox status, and protein expression, in achieving a higher level of specificity and efficacy.[4] For example, the use of light to control the reactivity of a prodrug has provided an external and orthogonal route of activation that is consistent throughout a broad range of applications.[5,6] Sadler et al. have shown that a noncytotoxic platinum(IV) diazido complex undergoes photoreduction and aquation following exposure to 325 nm light to form a cytotoxic platinum(II) complex,[5,7] a result that exemplifies the potential of utilizing light in prodrug strategies for transition metal-based therapeutics.

Nanomaterials have been studied extensively in prodrug applications using energy deposition strategies, including light activation.[8,9] Recently, colloidal quantum dots (QDs) have been shown to initiate photoreduction of Pt(IV) complexes to form potentially cytotoxic Pt(II) complexes through photoinduced electron transfer (PET) following photoexcitation at 615 nm.[10] The wavelength of light that initiates PET and subsequent Pt(IV) reduction is within a favorable range (600−1300 nm) for maximal tissue depth penetration for *in vivo* applications.[11] QDs possess highly tunable electrochemical and spectroscopic properties with excitonic transitions in the low-energy visible and near-infrared (NIR) regions.[12,13] In addition, QDs have high two-photon cross-sectional efficiencies that surpass those of traditional organic dyes.[14,15] Properties such as water solubility, cellular uptake, and selective accumulation in malignant tumors have been tuned to achieve superior biocompatibility.[16−19] These attributes make QDs favorable

**Received:** June 27, 2013
**Revised:** August 6, 2013
**Published:** August 9, 2013

   dx.doi.org/10.1021/ja4065393 | J. Am. Chem. Soc. 2013, 135, 13162−13167

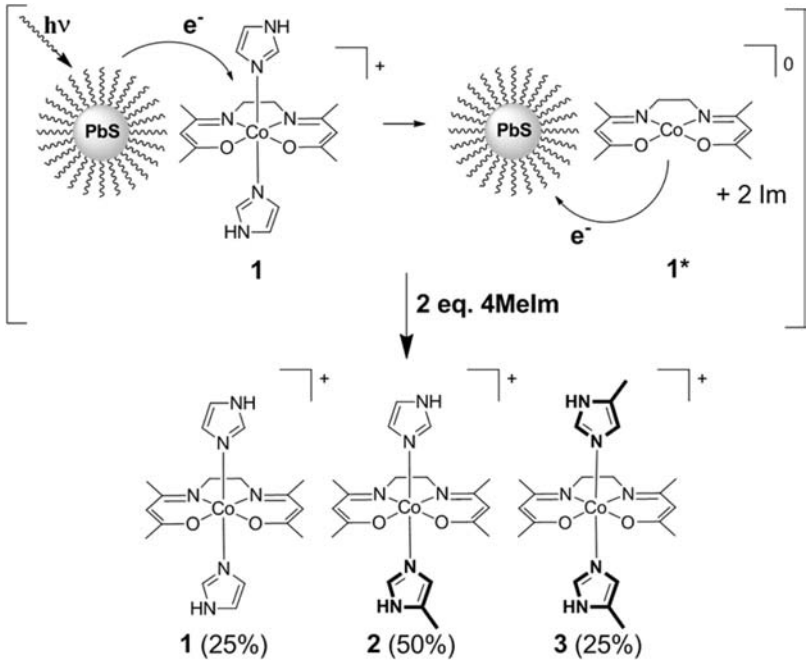


**Figure 1.** Co(acacen)$(Im)_2$ (**1**) adsorbs to the PbS QD surface, and PET occurs from the PbS QD to **1**, increasing the propensity for axial ligand dissociation (**1***). Oxidation back to Co(III) provides open coordination sites in the axial positions for the incoming ligand (here, 4MeIm) to form a mixture of three species (**1**–**3**) in relative abundances of 25, 50, and 25%, respectively.

candidates as photosensitizers for accessing multiple redox states of metal-based therapeutics in prodrug designs.

Cobalt(III) Schiff base [Co(III)-SB] complexes of the equatorial tetradentate ligand bis(acetylacetone)-ethylenediimine (acacen) are known to be potent inhibitors of a wide array of zinc-dependent proteins, including thermolysin, $\alpha$-thrombin, and matrix metalloproteinase-2.[20−23] Modification of the acacen backbone to incorporate biomolecular targeting moieties (such as oligonucleotides) has been shown to selectively target zinc finger transcription factors Sp1, Ci, and the Snail family.[24−26] Evidence suggests the inhibition activity is due to disruption of the protein structure by coordination of Co(III) to active-site histidine residues.[27−29] This coordination event occurs via a dissociative ligand exchange and is strongly dependent on the nature of the axial ligands present on the Co(III)-SB complex. Selective enzyme inhibition is observed when the axial positions are occupied by either sterically hindered 2-methylimidazole or labile amine ligands. In contrast, complexes with substitutionally inert axial ligands, such as imidazole (Im) or 4-methylimidazole (4-MeIm), are poor protein inhibitors. In general, the coordination behavior of cobalt Schiff base complexes is dependent on the oxidation state of the metal ion. Because of the redox properties of cobalt, axial ligand coordination of Co(II)-SB complexes has an increased propensity for dissociation.[27]

Here we describe a substitutionally inert Co(III)-SB complex, Co(acacen)$(Im)_2$ (**1**). Photoinduced electron transfer from a photosensitizer (a colloidal PbS QD with a radius between 1.5 and 1.7 nm, depending on the synthetic batch) reduces a Co(III)-SB complex to a Co(II)-SB complex, where the electron in the Co(II) occupies the antibonding $d_{z^2}$ orbital, creating a high-spin $d^7$ electronic configuration. The high-spin Co(II) complex has a higher axial ligand reactivity than the Co(III)-SB complex, so PET promotes axial ligand dissociation (**1***).[27,30] Subsequent charge recombination oxidizes the Co(II) center back to Co(III), providing an active Co(III)-SB complex with open axial coordination sites for essential His residues (Figure 1). The PbS QD/Co(III)-SB complex system is therefore a potential redox-activated prodrug.

## RESULTS AND DISCUSSION

We synthesized several batches of NIR light-absorbing PbS QDs with a first excitonic absorption between ∼900 and 1000 nm (see the Supporting Information); this absorption corresponds to core radii of 1.5−1.7 nm.[31] We selected PbS QDs for their tunable, size-dependent band-gaps in the range of 850−2100 nm, within the phototherapeutic window of biological tissue.[32,33] The Co(III)-SB complexes were synthesized and characterized according to literature procedures (see the Supporting Information). To prepare the PbS QD/Co(III)-SB complex samples, we transferred a methanolic solution of the Co(III)-SB complex into a scintillation vial and dried it under nitrogen before adding $1.4 \times 10^{-5}$ M PbS QDs in $CHCl_3$. The vial was shaken until the Co(III)-SB complex was dissolved, and the solution was allowed to equilibrate for 24 h before measurements were taken.

Reduction of the Co(III)-SB complex requires PET from the lowest unoccupied molecular orbital (LUMO) of the QD (populated by photoexcitation) to the LUMO of the Co(III)-SB complex. On the basis of ultraviolet photoemission measurements of the electronic structure of the QD[13] and cyclic voltammetry of the Co(III)-SB complex,[27] we estimate the driving force for the PET reaction to be ∼100 meV for QDs in this range of radii. We observe a quenching of the PL of the PbS QDs (upon excitation at 850 nm) with an increasing concentration of added Co(III)-SB complex (Figure 2A), consistent with electron transfer from the excitonic state of the QD. Figure 2B shows the PL intensity of each PbS QD/Co(III)-SB complex mixture relative to that of the QD sample alone ($PL/PL_0$) as a function of the concentration of added Co(III)-SB complex. As expected, we observe a decrease in PL


dx.doi.org/10.1021/ja4065393 | J. Am. Chem. Soc. 2013, 135, 13162−13167

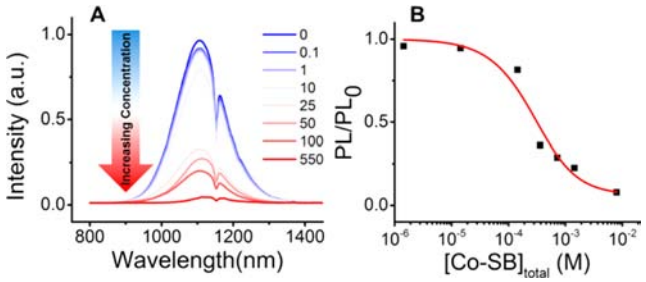


**Figure 2.** (A) Photoluminescence spectra showing the decrease in emission intensity of $1.4 \times 10^{-5}$ M PbS QDs in $CHCl_3$ upon addition of an increasing concentration of **1**. The legend indicates the number of molecules of **1** added per QD in the mixture, which we allowed to equilibrate for 24 h before recording the spectra. (B) Fraction of PL intensity remaining in the QD sample after addition of various concentrations of **1**, calculated by integrating the peaks in panel A. The fit to this data (red line) yields a saturated surface coverage of 2.5 Co(III)-SB complexes per QD, as described in the text.

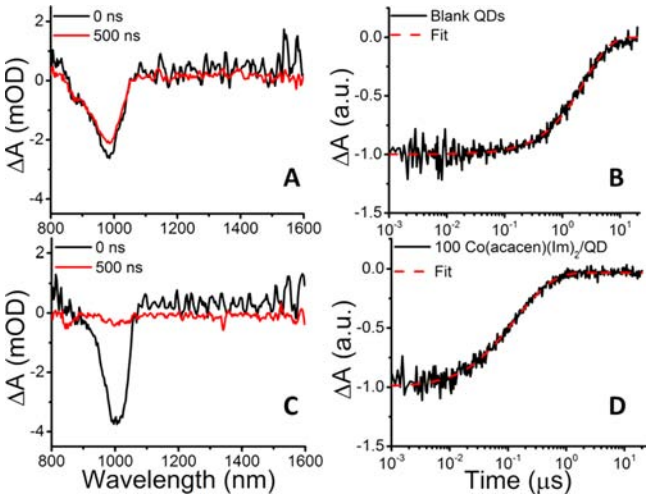


**Figure 3.** TA spectra of PbS QDs ($r$ = 1.7 nm) in $CHCl_3$ immediately after excitation (black) and after a 500 ns delay (red), showing the evolution of the ground state bleach at 1000 nm for samples without added **1** (A) and for samples containing 100 molecules of **1** added per QD (C). (B and D) Kinetic traces acquired at the peak of the ground state bleach for the same two samples. These traces show the dynamics of exciton decay. Dashed red lines are fits to the kinetic data, as described in the text. Without added Co(III)-SB, the exciton decays in 2.5 $\mu$s (Figure 3B). The intrinsic electron transfer rate between PbS QDs and the Co(III)-SB, obtained from the kinetic trace in Figure 3D is 125 ns.

intensity with an increasing concentration of Co(III)-SB complex until the PL of the QDs is completely quenched.

The degree to which an adsorbate quenches the PL of a dispersion of QDs by PET, $PL/PL_0$, is directly related to the average number of quenchers adsorbed in electron transfer-active geometries, if we can reasonably assume that the PET process quantitatively outcompetes other decay processes for the photoexcited electron in the QD. This assumption is reasonable in the case of PbS QDs, for which the electron decays with a time constant of ~3 $\mu$s in the absence of a quencher.[34,35] The model relating $PL/PL_0$ to the maximal (saturated) surface coverage of the Co(III)-SB complex on the QD and the adsorption equilibrium constant, $K_{ads}$, is detailed in the Supporting Information and elsewhere.[35] The red line in Figure 2B shows the fit of this model to the $PL/PL_0$ data. Through this analysis, we found that the maximal surface coverage of Co(III)-SB complexes per QD, $\theta_{max}$, is 2.5 (this number will vary with the intramolecular structure of the ligand coating on the QDs), and the equilibrium adsorption constant ($K_{ads}$) equals $1.1 \times 10^3$ $M^{-1}$ for the QD/Co(III)-SB complex system in $CHCl_3$. These results are consistent with the physisorption observed in other QD/molecule systems.[36,37]

Figure 3A shows the transient absorption (TA) spectrum of $1.4 \times 10^{-5}$ M PbS QDs in $CHCl_3$ immediately after photoexcitation at 850 nm (black) and after a 500 ns delay (red). Details of the TA experimental apparatus can be found elsewhere.[37] The negative feature at 1000 nm is the bleach of the ground state absorption of the QD, which decays with time, reflecting the depopulation of charge carriers (electron and/or hole) from their respective band-edges.

Depopulation of charge carriers occurs through exciton recombination or charge transfer to available trap states or molecular redox centers, like the Co(III)-SB complex. Figure 3B shows that, for the PbS QD sample without added **1**, a single-exponential function with a time constant of 2.5 $\mu$s (convoluted with an instrument response function) is adequate for fitting the kinetic trace for the ground state bleach recovery that we extracted from the TA spectrum at 1000 nm. Previous work has demonstrated that the observed rate constant for electron transfer from a QD to a molecular acceptor, $k_{eT,obs}$, increases linearly with the number of acceptors adsorbed per QD, $n$, as $k_{eT,int} = nk_{eT,obs}$,[37−39] where $k_{eT,int}$ is the intrinsic electron transfer rate constant, the rate constant observed if every QD that participates in electron transfer has exactly one adsorbed quencher. We found $k_{eT,int}$ by fitting the kinetic trace for the ground state bleach recovery in the sample of PbS QDs with added **1** (Figure 3D) with eq 1, where OD is the observed optical density at the wavelength of the ground state bleach

$$\Delta OD = IRF\{A_{eT}[1 + (e^{-k_{eT,int}t} - 1)\theta]^N + A_{CR}e^{-k_{CR}t}\} \quad (1)$$

(1000 nm), IRF is the instrument response function, $\theta$ is the average fractional surface coverage of the Co(III)-SB complex on the QD [obtained from $PL/PL_0$ (Figure 2)], $N$ is the total number of potential adsorption sites (empty or filled by native oleate ligands) per QD, $k_{CR}$ is the concentration-independent charge recombination rate constant, and $A_i$ is the amplitude of the relaxation pathway with rate constant $k_i$. The bracketed term accounts for electron transfer to the Co(III)-SB complex, which, as we assert in this model, is distributed on the surface of QDs according to a binomial distribution. The exponential function outside the bracket accounts for the recovery of the bleach caused by recombination of the transferred electron with a band-edge hole in the QD. The Supporting Information contains a derivation of eq 1. This process yields $(k_{eT,int})^{-1}$ = 125 ns and $(k_{CR})^{-1}$ = 258 ns. We show that the observed rate constant reflects PET within an adsorbed QD/Co(III)-SB complex, rather than PET rate-limited by diffusion of a quencher to the QD, in the Supporting Information. The Supporting Information also describes PL and TA experiments conducted with PbS QDs bound to a Co(III)-SB complex in which the native Im ligands have been replaced with *N*-methylimidazole (NMeIm). Addition of NMeIm to the Co(III)-SB complex increases the reduction potential of Co(III) to Co(II) by ~100 meV.[27] Consistent with our proposed electron transfer mechanism, treatment of the QDs with the $(NMeIm)_2$ complex quenches the PL of the QDs less


dx.doi.org/10.1021/ja4065393 | J. Am. Chem. Soc. 2013, 135, 13162−13167

efficiently and results in a slower excitonic decay than treatment of the QDs with the $(Im)_2$ complex. We observe no quenching of the QDs' PL upon addition of the acacen molecule [with no redox-active Co(III) center]. While these experiments support electron transfer as the primary mechanism for accelerated excitonic decay upon addition of the Co-SB complex, we cannot conclusively determine whether additional charge carrier trapping pathways also become available due to reconstruction of the QD's surface by the complex. Electron and hole trapping to surface states generally occurs on the time scale of picoseconds to hundreds of picoseconds, however, and we observe no exciton dynamics on that time scale.

Previous studies have shown that **1** in the presence of 2 equiv of 4MeIm forms a mixture of three species (**1**–**3**) in relative abundances of 25, 50, and 25%, respectively (Figure 1). The equilibrium bond distribution is 50% Co–Im bonds and 50% Co–4MeIm bonds.[28] We investigated the effect of PET on the axial ligand reactivity of **1** by monitoring the rate of the ligand displacement reaction for mixtures of **1**, 4MeIm, and PbS QDs with and without photoactivation of the PET process. We added 2 equiv (3.5 mM) of the competitive ligand, 4MeIm, to mixtures of PbS QDs ($1.4 \times 10^{-5}$ M) and **1** (1.7 mM) in $CDCl_3$ and monitored the axial ligand substitution reaction, specifically the decrease in the concentration of Co–Im bonds (Figure 4) and the increase in the concentration of Co–4MeIm bonds (Figure 4, inset), by $^1$H NMR spectroscopy.

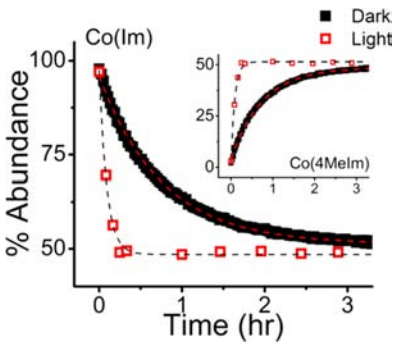


**Figure 4.** Abundance of imidazole bound to Co ["Co(Im)"] and 4MeIm bound to Co ["Co(4MeIm)"] (inset) in mixtures of $1.4 \times 10^{-5}$ M PbS QDs, 1.7 mM **1**, and 3.5 mM 4MeIm, where the mixtures were monitored by NMR in the dark (filled black squares) and under illumination (empty red squares) with light from a 75 W halogen lamp passed through a 400 nm long-pass filter. PET from the photoexcited QDs decreases the first order time constant for axial ligand substitution from 45 to 5.5 min.

We photoactivated the PbS QD/Co(III)-SB system by illuminating it in the NMR tube with a 75 W halogen lamp using a 400 nm long-pass filter, to photoexcite the PbS QDs but not the Co(III)-SB complex, while the contents were being stirred. We acquired the NMR spectrum of the reaction mixture after illumination for 0, 5, 10, 15, 20, 60, 90, 120, 150, and 180 min. With exposure to light, the axial ligand substitution reaction achieves the expected equilibrium state with a time constant of 5.5 min (Figure 4, empty red squares). We compared this time constant to that for a PbS QD/Co(III)-SB complex system with 2 equiv of 4MeIm, prepared under conditions identical to those used for the first sample, but monitored in the dark. To simulate the local heating of the first sample by the halogen lamp (which, we measured, heated the sample to 30 °C), we held this control sample at 30 °C during the NMR measurement. For the control sample, the axial ligand substitution reaction achieves its expected equilibrium state with a time constant of 45 min (Figure 4, filled black squares). These studies demonstrate that PET from the QD to the Co(III)-SB complex increases the rate of axial ligand substitution of **1** with 4MeIm by a factor of 8.2.

The high-energy photons with which we photoexcited the samples for the NMR experiment create electronically "hot" (above band-edge) carriers that relax to the band-edge states through several mechanisms, including phonon emission, which may cause local heating in the sample. The ligand substitution rate for Co-SB complexes does increase with temperature;[28] however, given the known temperature dependence of the Im–4MeIm equilibration rate in water,[28] the difference in energy between the average excitation photon used in the NMR experiment (2.07 eV) and the band-edge of the QDs (1.24 eV), and the heat capacity of lead sulfide, we estimate that perfect heat transfer from the QD to the Co(III)-SB complex would increase the temperature of the PbS lattice by only ~3 °C and increase the ligand substitution rate by a factor of 2–3. This value represents an upper bound, assuming that all excess energy is converted to heat, that the heat is transferred to the Co(III)-SB complex without loss, and that the Co(III)-SB complex does not dissipate heat itself. We are therefore confident that electron transfer to Co(III) is the primary mechanism for acceleration of axial ligand ejection.

## CONCLUSION

In summary, we have shown that selective photoexcitation of PbS QDs within mixtures of the QDs and $Co(acacen)(Im)_2$ increases the axial ligand reactivity of the Co(III)-SB complex, such that substitution of Im ligands with the His mimic 4MeIm occurs with a rate that is faster by a factor of >8 than in reaction mixtures that have not been photoactivated. We propose that the mechanism for this observation is electron transfer from the PbS QDs to Co(III), given that (i) the dissociation of axial ligands is a documented and well-understood consequence of reduction of Co(III) to Co(II) in this Co(III)-SB complex,[27] (ii) electron transfer from the bottom of the conduction band of PbS QDs of this size to Co(III) is energetically favorable by ~100 meV while energy transfer is not thermodynamically possible, (iii) addition of the Co(III)-SB complex to the QDs quenches their PL while exposure of the QDs to the acacen molecule without the redox-active Co(III) center does not quench their PL, and (iv) increasing the reduction potential of the Co(III) center within the Co(III)-SB complex by changing the axial ligand makes the Co(III)-SB complex a less efficient quencher of the PL of the QDs. Although, for the sake of convenience, we used a broad-spectrum light source in this proof-of-principle experiment, the creation of excitons in PbS QDs requires only NIR light.

Our measured time constant for axial ligand exchange of 5.5 min for the illuminated sample does not represent an intrinsic limit to the efficiency of ligand exchange for two main reasons. (i) In our study, the sample geometry was optimized ad hoc for the NMR experiment, but we can increase the axial ligand reactivity by optimizing illumination conditions such that all regions of the sample receive the maximal photon flux without photodegradation of the material. (ii) The PbS QDs used in this study are coated with a layer of oleate ligands that maximize the dispersibility of the QDs in organic solvents, to probe the physical parameters between the QD and the Co(III)-SB complex. We can improve the electronic coupling


dx.doi.org/10.1021/ja4065393 | J. Am. Chem. Soc. 2013, 135, 13162–13167

between the QD and the Co(III)-SB complex by using a QD coating that minimizes steric repulsion at the surface of the QD or by functionalizing the Co(III)-SB complex such that it can more closely approach the QD. For example, the Supporting Information describes a QD/Co(III)-SB complex system in which the Co(III)-SB complex can chemisorb to the surface of the QDs with a carboxyl group; for this system, we measured an intrinsic PET time of 2.2 ns, a value that is a factor of 50 faster than that of the QD/Co(acacen)$(Im)_2$ system described above. The labile axial ligands of this complex make it unsuitable for prodrug applications; however, the system represents a strategy for increasing the PET yield in these systems, if necessary. We have not yet determined the effect of the QD or its coating on the ability of a protein to bind to the axial position of the Co(III)-SB complex, but previous studies have shown that CdSe/ZnS QDs functionalized with peptides bind efficiently to streptavidin and other proteins.[40,41]

Our results offer a unique route for light activation of a Co(III)-SB protein inhibitor via NIR excitation and suggest that the development of inorganic therapeutic agents may be specifically coupled to a biologically active site by cooperative redox binding ligation. We expect that mechanisms of the phenomena described in this text are also applicable under biologically relevant conditions. Translation of this system to aqueous conditions involves exchanging the ligands on the particles for water-solubilizing ligands, which can be designed to maintain the absorption cross section of the QDs[16] and the lifetime of the QD excited state;[42] thus, we expect electron transfer to outcompete alternative relaxation mechanisms under aqueous conditions, as it does in organic solvents. Additionally, exchange of electrons between the QD and the complex apparently requires only physisorption of the donor and acceptor, which is achievable under aqueous conditions by adjusting the surface chemistry of the particles. Future studies will focus on fine-tuning the system to achieve biocompatibility through improving water solubility, cellular uptake, and selective accumulation in malignant tumors.

## ■ ASSOCIATED CONTENT

### Ⓢ Supporting Information

Experimental details, formulation and justification for eq 1, additional electron transfer-related calculations, and data from additional control experiments. This material is available free of charge via the Internet at http://pubs.acs.org.

## ■ AUTHOR INFORMATION


### Corresponding Authors

e-weiss@northwestern.edu
tmeade@northwestern.edu


### Author Contributions

M.D.P. and R.J.H. contributed equally to this work.

### Notes

The authors declare no competing financial interests.

## ■ ACKNOWLEDGMENTS

Research supported as part of the Argonne-Northwestern Solar Energy Research Center (ANSER), an Energy Frontier Research Center funded by the U.S. Department of Energy (DOE), Office of Science, Basic Energy Sciences (BES), via Grant DE-SC0001059 (electron transfer and NMR studies), and by the National Institutes of Health's Center of Cancer Nanotechnology Excellence initiative of National Cancer Institute via Grant U54CA151880, National Institutes of Health of National Cancer Institute via Grant RO3CA167715, and the Rosenberg Cancer Foundation (synthesis and NMR studies). The authors thank Ms. Marie C. Heffern and Dr. Natsuho Yamamoto for helpful discussions.

## ■ REFERENCES


(1) Zhang, C. X.; Lippard, S. J. *Curr. Opin. Chem. Biol.* **2003**, *7*, 481.
(2) Hambley, T. W. *Science* **2007**, *318*, 1392.
(3) Wang, D.; Lippard, S. J. *Nat. Rev. Drug Discovery* **2005**, *4*, 307.
(4) van Rijt, S. H.; Sadler, P. J. *Drug Discovery Today* **2009**, *14*, 1089.
(5) Farrer, N. J.; Woods, J. A.; Munk, V. P.; Mackay, F. S.; Sadler, P. J. *Chem. Res. Toxicol.* **2010**, *23*, 413.
(6) Graf, N.; Lippard, S. J. *Adv. Drug Delivery Rev.* **2012**, *64*, 993.
(7) Farrer, N. J.; Woods, J. A.; Salassa, L.; Zhao, Y.; Robinson, K. S.; Clarkson, G.; Mackay, F. S.; Sadler, P. J. *Angew. Chem., Int. Ed.* **2010**, *49*, 8905.
(8) Caruthers, S. D.; Wickline, S. A.; Lanza, G. M. *Curr. Opin. Biotechnol.* **2007**, *18*, 26.
(9) Nie, S.; Xing, Y.; Kim, G. J.; Simons, J. W. *Annu. Rev. Biomed. Eng.* **2007**, *9*, 257.
(10) Blanco, N. G.; Maldonado, C. R.; Mareque-Rivas, J. C. *Chem. Commun.* **2009**, 5257.
(11) Szaciłowski, K.; Macyk, W.; Drzewiecka-Matuszek, A.; Brindell, M.; Stochel, G. *Chem. Rev.* **2005**, *105*, 2647.
(12) Hines, M. A.; Scholes, G. D. *Adv. Mater.* **2003**, *15*, 1844.
(13) Jasieniak, J.; Califano, M.; Watkins, S. E. *ACS Nano* **2011**, *5*, 5888.
(14) Pu, S.-C.; Yang, M.-J.; Hsu, C.-C.; Lai, C.-W.; Hsieh, C.-C.; Lin, S. H.; Cheng, Y.-M.; Chou, P.-T. *Small* **2006**, *2*, 1308.
(15) Makarov, N. S.; Drobizhev, M.; Rebane, A. *Opt. Express* **2008**, *16*, 4029.
(16) Larson, D. R.; Zipfel, W. R.; Williams, R. M.; Clark, S. W.; Bruchez, M. P.; Wise, F. W.; Webb, W. W. *Science* **2003**, *300*, 1434.
(17) Gao, X.; Cui, Y.; Levenson, R. M.; Chung, L. W. K.; Nie, S. *Nat. Biotechnol.* **2004**, *22*, 969.
(18) Duan, H.; Nie, S. *J. Am. Chem. Soc.* **2007**, *129*, 3333.
(19) Cai, W.; Shin, D.-W.; Chen, K.; Gheysens, O.; Cao, Q.; Wang, S. X.; Gambhir, S. S.; Chen, X. *Nano Lett.* **2006**, *6*, 669.
(20) Harney, A. S.; Sole, L. B.; Meade, T. *JBIC, J. Biol. Inorg. Chem.* **2012**, *17*, 853.
(21) Takeuchi, T.; Bottcher, A.; Quezada, C. M.; Meade, T. J.; Gray, H. B. *Bioorg. Med. Chem.* **1999**, *7*, 815.
(22) Takeuchi, T.; Böttcher, A.; Quezada, C. M.; Simon, M. I.; Meade, T. J.; Gray, H. B. *J. Am. Chem. Soc.* **1998**, *120*, 8555.
(23) Heffern, M. C.; Yamamoto, N.; Holbrook, R. J.; Eckermann, A. L.; Meade, T. J. *Curr. Opin. Chem. Biol.* **2013**, *17*, 189.
(24) Harney, A. S.; Lee, J.; Manus, L. M.; Wang, P.; Ballweg, D. M.; LaBonne, C.; Meade, T. J. *Proc. Natl. Acad. Sci. U.S.A.* **2009**, *106*, 13667.
(25) Harney, A. S.; Meade, T. J.; LaBonne, C. *PLoS One* **2012**, *7*, e32318.
(26) Hurtado, R. R.; Harney, A. S.; Heffern, M. C.; Holbrook, R. J.; Holmgren, R. A.; Meade, T. J. *Mol. Pharmaceutics* **2012**, *9*, 325.
(27) Böttcher, A.; Takeuchi, T.; Hardcastle, K. I.; Meade, T. J.; Gray, H. B.; Cwikel, D.; Kapon, M.; Dori, Z. *Inorg. Chem.* **1997**, *36*, 2498.
(28) Manus, L. M.; Holbrook, R. J.; Atesin, T. A.; Heffern, M. C.; Harney, A. S.; Eckermann, A. L.; Meade, T. J. *Inorg. Chem.* **2013**, *52*, 1069.
(29) Matosziuk, L. M.; Holbrook, R. J.; Manus, L. M.; Heffern, M. C.; Ratner, M. A.; Meade, T. J. *Dalton Trans.* **2013**, *42*, 4002.
(30) Ware, D. C.; Wilson, W. R.; Denny, W. A.; Rickard, C. E. F. *Chem. Commun.* **1991**, 1171.
(31) Cademartiri, L.; Montanari, E.; Calestani, G.; Migliori, A.; Guagliardi, A.; Ozin, G. A. *J. Am. Chem. Soc.* **2006**, *128*, 10337.
(32) Tromberg, B. J.; Shah, N.; Lanning, R.; Cerussi, A.; Espinoza, J.; Pham, T.; Svaasand, L.; Butler, J. *Neoplasia* **2000**, *2*, 26.
(33) Boulnois, J.-L. *Lasers in Medical Science* **1986**, *1*, 47.

(34) Tachiya, M. *Chem. Phys. Lett.* **1975**, *33*, 289.
(35) Morris-Cohen, A. J.; Vasilenko, V.; Amin, V. A.; Reuter, M. G.; Weiss, E. A. *ACS Nano* **2012**, *6*, 557.
(36) Donakowski, M. D.; Godbe, J. M.; Sknepnek, R.; Knowles, K. E.; Olvera de la Cruz, M.; Weiss, E. A. *J. Phys. Chem. C* **2010**, *114*, 22526.
(37) Morris-Cohen, A. J.; Frederick, M. T.; Cass, L. C.; Weiss, E. A. *J. Am. Chem. Soc.* **2011**, *133*, 10146.
(38) Song, N.; Zhu, H.; Jin, S.; Zhan, W.; Lian, T. *ACS Nano* **2011**, *5*, 613.
(39) Rodgers, M. A. J.; Da Silva E Wheeler, M. F. *Chem. Phys. Lett.* **1978**, *53*, 165.
(40) Pinaud, F.; King, D.; Moore, H.-P.; Weiss, S. *J. Am. Chem. Soc.* **2004**, *126*, 6115.
(41) Goldman, E. R.; Anderson, G. P.; Tran, P. T.; Mattoussi, H.; Charles, P. T.; Mauro, J. M. *Anal. Chem.* **2002**, *74*, 841.
(42) Wuister, S. F.; de Mello Donegá, C.; Meijerink, A. *J. Phys. Chem. B* **2004**, *108*, 17393.